Precise Georeferencing of RGB and Multispectral Drone Images without Ground Control Points

José A. Gonçalves 1,2 *, Manuel Meyer 1,2, Ana Bio 2

¹ University of Porto, Science Faculty, Rua Campo Alegre, 4169-007 Porto, Portugal – jagoncal@fc.up.pt
² CIIMAR - Terminal de Cruzeiros de Leixões, 4450-208 Matosinhos, Portugal

Key words: Drone, image orientation, camera calibration, GNSS, multispectral.

ABSTRACT

Drones equipped with multispectral cameras are increasingly used in environmental studies. These surveys often take place in challenging locations such as mudflats, where marking and surveying ground control points (GCPs) is difficult, making the use of RTK-enabled drones essential. This paper analyses the achievable accuracy of orthomosaics (RGB and multi-spectral) and digital elevation models (DEMs) obtained with a drone, in order to carry regular surveys in estuarine areas in northern Portugal and Galicia, Spain. Accurate geolocation, particularly in the horizontal component, is crucial for combining data from different epochs, often under significantly changing conditions. Vertical accuracy is also important to assess tidal effects. In this study, a DJI Mavic 3M drone was used. Images were captured with a nadir orientation and supplemented with a final strip taken with the camera tilted, to optimize focal length self-calibration. After 21 survey flights, the stability of the interior orientation parameters was evaluated. The focal length varied within a range of 9 pixels, with a standard deviation of 2.2 pixels (0.06% of the focal length). Given the open question of whether there exists a single set of optimal calibration parameters for all cases, or whether, for example, due to environmental factors, the parameters, particularly the focal length, may vary, tests were conducted in a built-up area of approximately 30 hectares, where many GCPs could be surveyed. It was observed that each flight should have its calibration recalculated. The results showed that calibration based solely on the inclusion of oblique images and without the use of control points produced good results, with horizontal errors at the level of the image resolution and vertical error twice as that. The photogrammetric processing of the multispectral bands was carried out separately, and it was possible to conclude that georeferencing with positional accuracy comparable to the ground resolution can also be achieved, when rolling shutter compensation is applied. Results proved that the methodology followed for estuary surveys is appropriate to achieve results with accurate geolocation.

1. INTRODUCTION

Currently, drones allow for the acquisition of ultra-highresolution imagery that can be used in environmental studies, particularly when they capture not only RGB bands but also nearinfrared bands. These data enable highly localized studies that require the ability to distinguish small objects, thus complementing the use of satellite imagery (Piragnolo et al., 2018, Gati, 2024) or traditional aerial photography (Meyer et al., 2024). The analysis of drone-derived orthomosaics has been applied in studies of coastal and estuarine vegetation, through the calculation of vegetation indices or by applying image classification algorithms (Hamylton et al., 2020; Dolbeth et al., 2023; Meyer et al., 2023; Reinprecht, 2025). The need to combine data from different time periods or sensors requires precise georeferencing, which can usually be achieved through ground control points (GCPs). However, in certain environments, particularly in coastal regions, this may be challenging, making the use of drones equipped with Real Time Kinematic (RTK) satellite positioning (GNSS, Global Navigation Satellite Systems) highly advantageous (Taddia, 2019, Llabani & Kopliku, 2024).

The work described in this paper refers to a research project carried out in Portugal (Northern region) and Spain (Galicia), which investigates estuarine marsh vegetation due to its key role in carbon sequestration. As part of this project, a DJI Mavic 3 Multispectral drone is used to capture traditional colour images

⁽RGB) and multispectral (MS) images of estuaries during low tide periods. These areas contain various types of aquatic vegetation that are intended to be mapped and quantified. They also include extensive mudflats, mostly inaccessible, which pose significant challenges for drone-based surveys. Figure 1 shows the region and the study areas where drone surveys were done.

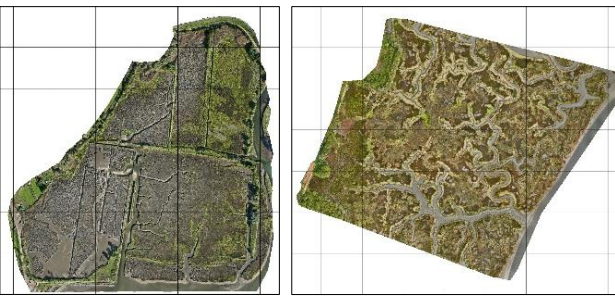


Figure 1. Location of the study areas (white dots) in North Portugal and Galicia, Spain.

Figure 2 shows two of the study areas, one in the estuary of River Lima (A), near the city of Viana do Castelo, and the other in Ria de Betanzos (B), near the city of Coruña.

^{*} Corresponding author

Accurate georeferencing is crucial in this study for two main reasons. First, the need to compare data from different sensors or different time periods, integrating raster images on a pixel-by-pixel basis, requires georeferencing errors to be limited to just a few pixels. In addition to demanding high positional accuracy in the horizontal component, the vertical component can also benefit from high accuracy. Image acquisition is typically carried out at very low tide, with most areas exposed and free of water. Using the stereoscopic coverage provided by the RGB images, it is possible to generate DEMs that allow for estimating vegetation height as well as predicting the time of vegetation submersion at high tide.



A – Estuary of Lima

B - Ria of Betanzos

Figure 2. Examples of two of the surveyed areas - A: Estuary of Lima River (Portugal), B: Ria de Betanzos (Spain)

Drone image georeferencing is typically achieved through GCPs placed in the area and surveyed using GNSS. In this case, however, such an approach is virtually impossible, and the use of a drone with RTK differential positioning was chosen. Since it was very difficult to have independent check points (ICPs) in the mapped areas, some uncertainty remained regarding potential georeferencing errors, both in the horizontal and vertical components. The main objective of this paper is to present the methods used to ensure accurate georeferencing of both RGB and multispectral images without the use of GCPs.

Although the drone provides highly accurate camera positioning, with standard deviations similar to ground sampling distance (GSD), this does not guarantee that the resulting georeferenced information will maintain the same accuracy. The challenge lies in the process of self-calibration of the interior orientation parameters, such as the lens focal length, for which only an approximate value is known. The flight planning software includes an option to acquire some images with the camera tilted, the "altitude optimization" option (DJI, 2022), which introduces a different ratio between focal length and camera-to-ground distance at the image centre, thus reducing the uncertainty in focal length estimation. This paper aims to assess whether this approach is sufficient, or whether additional steps such as camera pre-calibration are necessary.

2. MATERIAL AND METHODS

The work was carried out using a DJI Mavic 3 Multispectral drone, which includes two independent image sensors: a 20-megapixel RGB camera and a multispectral sensor composed of four cameras (5 megapixel), each dedicated to one spectral band. It also features an RTK GNSS receiver, which enables high-precision positioning and trajectory determination. Figure 3 shows the cameras (the MS system composed by 4 cameras, above the RGB camera), and the GNSS module, on top of the drone. The following sections describe these three system components and the aspects analysed in this paper.



Figure 3. A: MS system, with 4 cameras, on top, and RGB camera, below. B: GNSS module on top of the drone.

2.1 RGB Camera

The RGB camera uses a 4/3 CMOS sensor, approximately 17.7 mm by 13.3 mm in size, equipped with a 12.9 mm focal length lens (DJI, 2022). The pixel size is 3.36 microns, with a total resolution of 5280 by 3956 pixels (20 megapixels). When expressed in pixel units, the focal length is approximately 3713 pixels. The focal length, f, in pixels is used directly to calculate the GSD using the following formula:

$$GSD = \frac{H}{f} \tag{1},$$

where H is the flight altitude in meters. At an altitude of 110 meters, for example, the GSD is approximately 3 cm.

The images captured by the drone appear in the original sensor geometry, with some radial distortion. The metadata includes internal orientation parameters according to the Brown distortion model: focal length (f), principal point coordinates, (c_x, c_y) , radial distortion coefficients, (k_1, k_2, k_3) , and tangential distortion coefficients, (p_1, p_2) . These parameters, for the drone used, resulting from factory calibration, are listed in Table 1.

Parameter	Values
f	3713.3
c_x, c_y	+7.0, -8.7
k_1, k_2, k_3	-0.0113, +0.0149, -0.0271
p_{1}, p_{2}	+0.000000, -0.000086

Table 1 – interior orientation parameters included in the images metadata.

These parameters follow the format used by Metashape (Agisoft, 2025). Regarding the distortion components, radial distortion is relatively high, reaching up to 300 pixels at the edge of the diagonals. Tangential distortion, on the other hand, is very minor, remaining below 0.5 pixels. Figure 4 shows a plot of radial distortion (relative to the image centre) along the diagonal at various distances from the centre.

The RGB camera in this drone is identical to the one found in the Mavic 3 Enterprise model. It is worth noting that, among several RGB camera units examined, two from the Mavic 3E and two from the Mavic 3M, these internal parameters were identical across all units. The internal orientation parameters embedded in drone image metadata are considered as initial approximations and are adjusted during bundle adjustment through self-calibration, as discussed further in Section 2.3. The need for a careful camera calibration is critical in RTK drone processing (Gerke & Przybilla, 2016).

According to the manufacturer's documentation, the camera uses a mechanical shutter, allowing the entire image to be captured simultaneously. This prevents potential distortions that may occur with rolling shutter systems. The analyses presented in Section 3 evaluates the changes observed in the calibration parameters provided in the metadata.

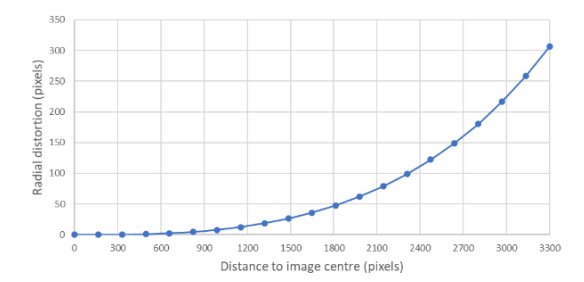


Figure 4. Radial distortion (y axis) along the semi-diagonal as a function of distance to image centre (x axis), all in pixel units.

2.2 MS Camera

The Mavic 3M drone contains, in its multispectral (MS) component, 4 cameras operating in the Green (G), Red (R), Rededge (RE), and Near Infrared (NIR) bands, centred respectively at wavelengths of 560, 650, 730, and 860 nm, with bandwidths of 32 nm, for G, R and RE, and 52 nm in the case of NIR. The sensors are 1/2.8-inch size, each with 5 MP resolution. The pixel size is 2 microns, and the lenses have a focal length of 4.34 mm. At a height of 110 meters, the GSD of the MS bands is 5 cm.

As with the RGB camera, calibration parameters are also known for each of the 4 cameras, which are embedded in the metadata and are used as initial approximations for self-calibration. These cameras feature an electronic shutter, so it is important to assess whether any geometric "rolling-shutter" effects occur and whether they should be corrected during the bundle adjustment process.

The distance between the most distant cameras (R and G) is only 3 cm. During processing, the Metashape software assumes a single position, which introduces a negligible error. A much more significant issue is that the optical axes of the 4 cameras are not parallel to each other. This means that the coverage of each of the 4 images is not the same. To ensure that the final orthorectified bands are correctly overlaid, Metashape selects one of the bands as the reference (master) and computes, for each of the other 3 (slave) bands, the rotation angles, *omega*, *phi*, and *kappa*, required to correctly orient them relative to the master band. It is also on the master band that tie point identification is performed for the image alignment phase.

One might consider using the RGB image as the master and all the MS bands as slaves. However, this is not possible because the acquisitions are not simultaneous. According to the metadata recorded in the images, there is a time difference of about 26 ms, which, given the drone's speed, results in a significant shift between projection centres (0.26 m at a speed of 10 m/s). Therefore, the processing must be done separately. First, the RGB images are processed to generate a DEM and an orthomosaic. Then, the MS images are aligned and orthorectified, using the previously extracted DEM, to directly produce an orthomosaic.

It is essential to evaluate the horizontal alignment between the RGB and MS orthomosaics. In cases where, for some reason, there is not a good match, it is always possible to use GCPs with horizontal coordinates read from the RGB orthomosaic and elevations obtained on the DEM.

2.3 GNSS RTK receiver

The drone is equipped with an RTK GNSS receiver capable of receiving satellite signals from all four constellations (GPS, GLONASS, BeiDou, and Galileo), at a frequency of 5 Hz. It can connect in real time to a GNSS base station to receive differential corrections and thus obtain highly accurate positional data at intervals of 0.2 seconds. Images are captured at different moments, and the exact time of each shutter trigger is recorded, allowing interpolation to that specific moment. Since the camera's projection centre is located in a different position, about 10 cm away, it is necessary to apply the lever-arm transformation involving the gimbal's attitude angles, which are measured by the drone

The camera position determined in this way will have an accuracy of a few centimetres, which is likely sufficiently precise for mapping purposes. The remaining external orientation parameters, the attitude angles, are not taken from the drone's attitude sensors, as they do not provide sufficient precision. The problem of determining these angles is solved in the photogrammetric processing phase known as image alignment, which involves a bundle adjustment, with the knowledge of the camera positions.

The computation of 3D ground coordinates of a point observed in two or more images is carried out through photogrammetric equations, which use both the external orientation parameters and the internal orientation parameters mentioned earlier. Since these internal parameters are only approximate values of the real ones, the processing includes a self-calibration procedure, in which they are adjusted simultaneously with the bundle adjustment. As previously mentioned, the focal length is a particularly sensitive parameter in self-calibration, since it is directly related to the flight height, that is, the vertical distance between the ground and the camera. Analysing expression (1), a small percentage variation in f is compensated by a proportionally small variation in H. Naturally, this alters the image geometry, but not significantly, and the resolution remains essentially the same. If we have a highly accurate camera position from RTK GNSS, this will affect altitude determination. Thus, when only vertical photos are available and the terrain elevation variation is much smaller than the flight height, the estimated focal length is subject to high uncertainty, as are the resulting altitude values.

The obvious way to mitigate this problem is by using GCPs. However, to try to avoid that, an alternative is to include oblique images in the flight coverage. For those images, the ground-to-camera distance at the image centre will be different, forcing the estimated focal length in the self-calibration to be closer to the real value. This option is available in the drone's flight planning software under the designation "Altitude optimization". In estuarine environments, this is especially useful due to the difficulty of establishing GCPs and because such terrain typically has very little elevation variation. The following tests aim to evaluate the quality of the external orientation parameters obtained using this approach.

2.4 Processing software

Regarding processing software, Agisoft Metashape (version 2.2) was used. This software applies largely automated methods to perform image alignment, DEM generation, and orthomosaic production. It is capable of correctly handling the involved data: 8-bit RGB images, 16-bit multispectral images (treated as a multi-camera system), and high-precision positioning data, where each measured coordinate includes an associated variance

that serves as a weight in the least-squares adjustment process (Agisoft, 2025).

3. RESULTS OF TESTS IMPLEMENTED

Flights were conducted in the study areas, located in estuaries, between September and November 2024. Each flight, lasting up to 20 minutes, resulted in several hundred photos, with some areas requiring more than one flight. Additionally, three more flights were carried out in June 2025 in estuarine areas in Portugal. For validation and calibration purposes, three flights were also conducted in December 2024 and June 2025 over a built-up area where many check points could be surveyed with GNSS. In total, 21 flights were performed, with an average of 530 images per flight. The following sections describe the analyses performed on these data, initially processed without GCPs. The RGB camera was also calibrated (section 3.2), with accurate GCPs, and the impact of this calibration on other flights, without GCPs, was assessed. Finally, the processing of the MS images is described (section 3.3), along with an evaluation of their spatial agreement with the RGB mosaic.

The drone was operated with a real-time connection to the nearest station of the CORS networks (Continuously Operating Reference Stations). The public networks available in Portugal and Spain are dense enough to ensure that, in most cases, the nearest station is within 30 km. In the surveys carried out in the estuaries in the calibration area, the largest distance to the nearest CORS station was 23 km. In all cases, phase ambiguity resolution was always achieved.

3.1 Processing without GCPs

In the flights over the estuaries, the possibility of collecting checkpoints was very limited, at most, only in boundary areas of the covered regions. In all flights, an oblique strip was included for altitude optimization, and the images were processed in the Metashape software without using control points, relying solely on the RTK camera positioning.

For performance evaluation purposes, the interior orientation parameters obtained were recorded. Table 2 presents a summary of the parameters obtained for the focal length and principal point position. Of the 21 flights considered, 16 were flown at an altitude of 70 meters and the remaining at 110 meters (resulting in RGB GSD of 2 and 3 cm, respectively). For each flight the camera interior parameters were exported and analysed. Table 2 contains the statistics of the parameters f and (c_x, c_y) , referring to the 21 flights performed. All values are in pixel units.

Parameter	Mean Value	Std. Dev.	Max - Min
f	3715.78	2.27	8.96
c_x	-18.18	0.31	1.00
c_{ν}	-45.38	0.27	1.03

Table 2 – Statistics of focal distance and principal point coordinates obtained in 21 flights. All values are in pixel units.

A high level of stability was observed in the obtained parameters, especially in the principal point position, with standard deviations of around 0.3 pixels in the two coordinates. The focal length showed greater variation, with a standard deviation around of 2.3 pixels, which corresponds to 0.06% of the estimated value. The difference between the maximum and minimum values was around 9 pixels. An error in focal length estimation has a direct impact on altitude calculation for DEM generation: an error of

one-pixel in focal length results in a systematic elevation error equal to 1 GSD (Stroner et al., 2021). For a GSD of 3 cm, the observed range of focal distances corresponds to a maximum elevation difference of 27 cm.

The distortion parameters are not presented in the table. However, it can be noted that for all flights they are very similar. Some comparison experiments using different parameters resulted in projections with average differences of less than half a pixel.

To gain more certainty regarding these questions, it was decided to do a camera calibration in a control area where it is possible to use marked points surveyed with GNSS.

3.2 Camera calibration with GCPs

In order to do a camera calibration, a location near the city of Coimbra, in Portugal, was selected. This is a built-up area, with approximately 30 hectares, and several roads with painted marks on the pavement. Some of these well-defined marks were initially used as check points. Figure 5 shows the area.



Figure 5. Image of the area used for control surveys, with the marked points for the reference survey.

A first flight was carried out in December 2024, considering pavement marks, such as corners of zebra crossings, as ICPs or GCPs. Later, due to concerns about the stability of the calibration, a new flight was conducted at the same location in June 2025. It was observed that, due to construction work, some of the pavement markings disappeared or were changed, so a third flight was carried out the following day. A total of 26 marks were painted on the pavement and sidewalks, of which two examples are shown in figure 6.





Figure 6. Examples of two marked GCPs.

Figure 5 shows the location of the 26 GCPs that were marked. They were surveyed using a triple-frequency GNSS receiver in RTK mode, connected to a CORS station located 18 km away. The estimated accuracy was 1 to 2 cm in the horizontal component and 2 to 3 cm in the vertical.

The following approach was adopted: the third flight was considered the reference flight and was adjusted using the GCPs. From this flight, an orthomosaic, a DEM, and a set of calibration

parameters were produced and used as a reference. The other two flights were processed without any GCPs in order to assess the results by comparing them with the reference data.

3.2.1 Results for the reference flight

The reference flight was processed in Agisoft Metashape, initially without GCPs, and including the oblique images. The 26 points were inserted in the project as ICPs and were marked in all images where they could be identified. Residuals result for the three coordinates, as well as root mean square errors (RMSE), which are presented in table 3. Then, the points were considered as GCPs, with the corresponding standard deviations, in order to consider correct observation weights. The bundle adjustment was recalculated, once again originating the RMSE of the residuals. Results of focal lengths and RMSE of the three coordinates (horizontal, X and Y, and vertical, H), in meters, are presented in table 3.

	No GCPs, oblique strip	Oriented with GCPs
Focal length	3713.98	3713.87
RMSE X	0.028	0.021
RMSE Y	0.024	0.019
RMSE H	0.047	0.029

Table 3 – results of adjustment first without GCPs and then with GCPs. *f* in pixels, RMSE in meters.

As can be observed, two very close focal lengths resulted. The errors obtained without GCPs are good. In the case of horizontal coordinates, the errors are similar to the GSD (3 cm) and in altitude, they are about 50% larger. In the case of using GCPs, the errors improve, as would be expected. For the intended use of estuary mapping, not using GCPs allows for adequate results.

3.2.2 Results for the other flights

The other two flights, one from June, the day before the reference flight, and the other from December 2024, did not include the marked GCPs used in the reference flight. These two flights were processed without GCPs, generating orthomosaics and DEMs. The horizontal and vertical accuracy was analysed by comparison with the orthomosaic and DEM generated from the reference flight. Based on a qualitative assessment, the horizontal agreement between the orthomosaics is very high. To quantify this small difference, 16 well-defined points, located in flat areas, were identified in the reference orthomosaic. Coordinates were measured on the other two orthomosaics, and errors were calculated. For the DEMs, the elevation at these 16 points was assessed in each DEM. Points were identified and coordinates were measured in QGIS software. Heights were extracted from the DEMs with the Point Sampling Tool plugin.

These two flights were processed including the oblique flight line, without GCPs, and with the camera calibration parameters free to be adjusted. A second run was performed, this time fixing the camera calibration parameters obtained from the reference flight (focal distance 3713.87 pixels). The test results for the January and June flights, with either free or fixed camera parameters, are listed in Table 4. In the case of the RMSE of the horizontal coordinates, the norm (square root of the sum of the squared RMSE values in X and Y) is presented. All the RMSE are in meters. Focal lengths are in pixel units.

	Flight of January		Flight of June	
Cam. calibration	Free	Fixed	Free	Fixed
Focal distance	3715.08	3713.87	3712.56	3713.87
RMSE XY	0.038	0.037	0.028	0.032
RMSE H	0.040	0.090	0.021	0.060
Std. Dev. H	0.017	0.020	0.036	0.033

Table 4 – Results of the processing of the January and June flights, with free calibration and with fixed calibration

These RMSE values were plotted in a bar graph (figure 7), expressed in GSD units, which in this case was 3.1 cm.



Figure 7. Graphical representation of RMSE values in terms of GSD.

It can be observed that, when the camera parameters are allowed to be adjusted, the resulting focal length differs by only 1 or 2 pixels compared to the pre-calibrated value. There is virtually no effect on the horizontal error. However, the vertical component is affected, with the RMSE increasing to nearly three times the value obtained with free calibration. The table also includes the standard deviation of the vertical errors, which is on the order of the image resolution. The reason is that using a fixed focal length introduces systematic altitude errors. The main conclusion is that, if accurate elevation information is desired, the focal length should be adjusted for each flight. In the case of the horizontal component, the effect is not significant.

Returning to the surveys carried out in the estuaries, error assessments were also conducted in the only locations where validation points were collected. In the Ria de Ramallosa, near city of Vigo, 9 points were surveyed on pavement markings along a road in the margin of the estuary (Figure 8A). Horizontal and vertical errors were: $RMSE_{XY} = 0.021 \, m$ and $RMSE_H = 0.039 \, m$.

In the Ria de Betanzos, 18 points were surveyed on a beach area, near to the mudflat (Figure 8B). In this case, only the vertical error could be assessed: $RMSE_H = 0.041 \ m$

In both cases, the GSD of the RGB image was 2.0 cm. The results are consistent with the trend of horizontal RMSE being around 1 GSD and vertical RMSE being higher, up to 2 GSD.

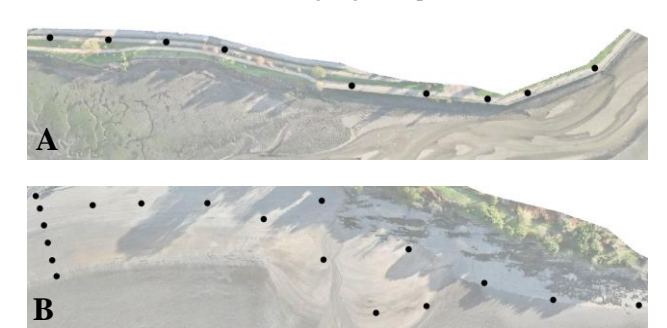


Figure 8. Estuary areas where check points (black dots) were surveyed: A – Ria de Ramallosa, B – Ria de Betanzos.

3.2.3 Processing of multi-spectral images

The processing of the MS images is done separately. All bands are loaded and identified as belonging to a "multi-camera system". One of the bands is chosen as the master, and tie points are detected on it for alignment. The oblique flight line is also considered for adjusting the calibration of each of the four lenses. Once the adjusted internal and external orientation parameters are obtained, it is possible to generate an orthomosaic for each of the bands, using the DEM previously extracted from the RGB images. Regardless of the accuracy of the camera position or the use of GCPs, the alignment of the bands will always be correct, as this is handled, as mentioned earlier, through the calculation of the relative orientation angles of each camera in relation to the master.

The aim of this part of the work is to assess the geolocation accuracy of the resulting orthomosaic, as was done with the RGB images. Here, it is also necessary to consider whether rolling shutter geometric effects are introduced. Agisoft Metashape includes the option to compensate for this effect, and processing was tested both with and without rolling shutter compensation.

The reference flight was processed, which includes 26 check points. These points were added to the project and marked as check points so that they would not influence the solution. They were identified in the images where visible, resulting in ground coordinates. The difference to GNSS coordinates originates residuals, from which the RMSE values were calculated. These RMSE values, obtained from the photogrammetry project, are presented in Table 5, both for processing with and without rolling-shutter compensation.

The orthomosaics were exported to QGIS, and the locations of the ICPs were also measured. The corresponding horizontal RMSE were obtained and are also presented in the table, for both cases.

Error	RS	ICP RMSE		
assessment	Comp.	X	Y	H
Photogrammetry	No	0.154	0.264	0.192
project	Yes	0.050	0.026	0.065
Orthomosaic	No	0.153	0.324	
	Yes	0.042	0.045	

Table 5 – RMSE values in the ICPs obtained from the photogrammetric project and from the orthomosaic, with and without rolling-shutter compensation. Units are meters.

Finally, figure 9 presents an example of a check point, shown over the RGB orthomosaic (A) and over the orthomosaics of a false color composite (IRG), obtained without (B) and with (C) rolling shutter compensation. Grid overlays have a spacing of 1 meter.

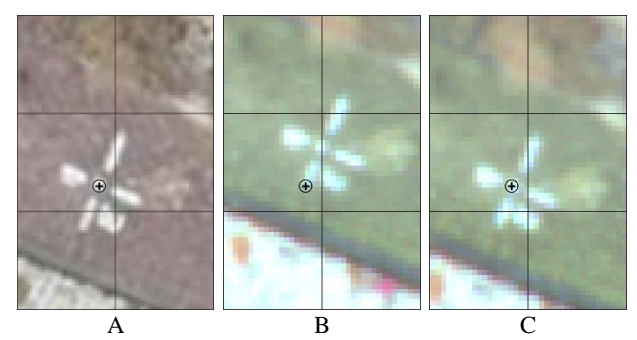


Figure 9. Example of a check point on the orthomosaics: $A-RGB,\,B-MS$ image without rolling shutter compensation, and C- with compensation.

Ignoring this effect would result in a displacement of many pixels, making integration with other data very inaccurate.

4. Conclusions

This study evaluated the georeferencing accuracy of RGB and multispectral drone imagery acquired with an RTK-enabled drone, without relying on GCPs. The results demonstrate that sub-decimetric accuracy can be achieved in horizontal positioning and acceptable precision in elevation, even under challenging environmental conditions such as estuarine mudflats where GCP placement is not feasible.

Tests across 21 flights showed that the interior camera parameters, particularly the focal length, exhibit good stability, with standard deviations below 0.1%. However, results from a controlled calibration area revealed that allowing the focal length to be freely adjusted for each flight yields better vertical accuracy, with RMSE values reduced by up to a factor of three compared to using fixed calibration parameters. This suggests that, despite the high quality of factory calibration, on-the-fly self-calibration using oblique imagery remains necessary, particularly when precise elevation data are needed.

For multispectral images, separate processing of the bands and the use of a master-slave camera model provided correct band alignment. However, rolling shutter effects were found to introduce significant geometric distortions, with RMSE errors reaching several pixels if not compensated. When rolling shutter correction was applied, RMSE values decreased to less than 0.05 m, corresponding to sub-GSD accuracy.

In conclusion, the combination of RTK GNSS positioning, strategic flight planning (including oblique strips), and careful photogrammetric processing, including rolling shutter compensation, makes it possible to generate high-quality georeferenced products without GCPs. This methodology is highly suitable for recurring surveys in difficult-to-access environments, enabling consistent and accurate monitoring of dynamic coastal and estuarine ecosystems.

Acknowledgements

This work was supported by the project CAPTA (0062_CAPTA_1_E), co-funded by the European Union through the Interreg VI-A Spain-Portugal (POCTEP) 2021-2027 programme, and partially supported by the Strategic Funding UIDB/04423/2020, UIDP/04423/2020 and LA/P/0101/2020 through national funds provided by the Portuguese Foundation for Science and Technology (FCT).

References

Agisoft (2025). Agisoft Metashape User Manual - Professional Edition, Version 2.2. Accessible on-line https://www.agisoft.com/pdf/metashape-pro_2_2_en.pdf

DJI (2022). DJI Mavic 3M Enterprise Multispectral User's Manual v1.0; 2022.12. Accessible on-line: https://dl.djicdn.com/downloads/DJI_Mavic_3_Enterprise/2022 1216/DJI_Mavic_3M_User_Manual_EN.pdf

Dolbeth, M., Costa, D. D. A., Meyer, M., Gonçalves, J. A., & Bio, A. (2023). Characterisation and Dynamics of an Emerging Seagrass Meadow. Remote Sensing, 15(16), 4086.

Gerke, M., & Przybilla, H. J. (2016). Accuracy analysis of photogrammetric UAV image blocks: Influence of onboard RTK-GNSS and cross flight patterns. Photogrammetrie, Fernerkundung, Geoinformation, 2016(1), 17-30.

Gati, B. (2024). Comparison of vegetation indices obtained by drone and satellite. In E3S Web of Conferences (Vol. 590, p. 01008). EDP Sciences.

Hamylton, S. M., Morris, R. H., Carvalho, R. C., Roder, N., Barlow, P., Mills, K., & Wang, L. (2020). Evaluating techniques for mapping island vegetation from unmanned aerial vehicle (UAV) images: Pixel classification, visual interpretation and machine learning approaches. International Journal of Applied Earth Observation and Geoinformation, 89, 102085.

Llabani, A., & Kopliku, N. (2024, April). Assessing the accuracy of UAV Systems in urban areas without Ground Control Points. In Proceedings of the 2024 7th International Conference on Geoinformatics and Data Analysis (pp. 1-6).

Meyer, M. D. F., Gonçalves, J. A., Cunha, J. F. R., Ramos, S. C. D. C. E. S., & Bio, A. M. F. (2023). Application of a multispectral UAS to assess the cover and biomass of the invasive dune species Carpobrotus edulis. Remote Sensing, 15(9), 2411.

Meyer, M. D. F., Gonçalves, J. A., & Bio, A. M. F. (2024). Using Remote Sensing Multispectral Imagery for Invasive Species Quantification: The Effect of Image Resolution on Area and Biomass Estimation. Remote Sensing, 16(4), 652.

Piragnolo, M., Lusiani, G., & Pirotti, F. (2018). Comparison of vegetation indices from RPAS and Sentinel-2 imagery for detecting permanent pastures. The International Archives of the Photogrammetry, Remote Sensing and Spatial Information Sciences, 42, 1381-1387.

Reinprecht, V., & Kieffer, D. S. (2025). Application of UAV Photogrammetry and Multispectral Image Analysis for Identifying Land Use and Vegetation Cover Succession in Former Mining Areas. Remote Sensing, 17(3), 405.

Štroner, M., Urban, R., Seidl, J., Reindl, T., & Brouček, J. (2021). Photogrammetry using UAV-mounted GNSS RTK: Georeferencing strategies without GCPs. Remote Sensing, 13(7), 1336.

Szypuła, B. (2024). Accuracy of UAV-based DEMs without ground control points. GeoInformatica, 28(1), 1-28.

Taddia, Y., Stecchi, F., & Pellegrinelli, A. (2019). Using DJI Phantom 4 RTK drone for topographic mapping of coastal areas. The International Archives of the Photogrammetry, Remote Sensing and Spatial Information Sciences, 42, 625-630.